

(Proposal to Jefferson Lab PAC 34)

Studies of the L-T Separated Kaon Electroproduction

Cross Section from 5-11 GeV

December 15, 2008

P. Bosted, S. Covrig, R. Ent, H. Fenker, D. Gaskell, T. Horn (co-spokesperson)¹

M.K. Jones, J. LeRose, D.J. Mack, G.R. Smith, S.A. Wood

Jefferson Lab, Newport News, Virginia

G.M. Huber (co-spokesperson), Z. Papandreou

University of Regina, Regina, Canada

W. Boeglin, P. Markowitz (co-spokesperson), B. Raue, J. Reinhold

Florida International University, Miami, Florida

F.J. Klein, P. Nadel-Turoński

The Catholic University of America, Washington, DC

A. Asaturyan, A. Mkrtchyan, H. Mkrtchyan, V. Tadevosyan

Yerevan Physics Institute, Yerevan, Armenia

D. Dutta

Mississippi State University, Mississippi State, MS

M. Kohl, P. Monaghan, L. Tang

Hampton University, Hampton, Virginia

D. Hornidge

Mount Allison University, Sackville, Canada

A. Sarty

Saint Mary's University, Halifax, Canada

E. Beise

University of Maryland, College Park, Maryland

G. Niculesu, I. Niculescu

James Madison University, Harrisonburg, Virginia

K. Aniol

California State University Los Angeles, Los Angeles, California

E. Brash

Christopher Newport University, Newport News, Virginia

V. Punjabi

Norfolk State University, Norfolk, Virginia

C.F. Perdrisat

2

College of William and Mary, Williamsburg, Virginia

Y. Ilieva

University of South Carolina, Columbia, South Carolina

F. Cusanno, F. Garibaldi, M. Iodice, S. Marrone

Istituto Nazionale di Fisica Nucleare, Italy

P.M. King, J. Roche

Ohio University, Athens, Ohio

¹ Contact person: hornt@jlab.org

The $p(e, e'K^+)\Lambda$ and $p(e, e'K^+)\Sigma^0$ reactions are important tools in our study of hadron structure. The flavor degree of freedom introduced with the addition of the strange quark provides important information for QCD model building, as well as for our improved understanding of the basic coupling constants needed in nucleon-meson and quark models. Despite these positive aspects, these reactions have been relatively unexploited to date because of the lack of the necessary experimental facilities. As a result, there are practically no L-T separation data for exclusive K^+ production from the proton above the resonance region.

With the higher beam energies and the new SHMS spectrometer planned for Hall C, we have the opportunity to dramatically improve upon this situation. This proposal has the following primary goals:

1. Studies of the Kaon Production Mechanism

Prior studies to determine whether the K^+ pole term dominates σ_L at low $-t$ have been complicated in their interpretation by potential resonance contributions. Questions, such as the roles of K and K^* t -channel exchanges, and the contributions of higher transitions on the corresponding Regge trajectories have been raised. Even the relative importance of σ_L compared to σ_T is not well understood due to the lack of sufficiently precise data. Furthermore, theoretical predictions for σ_T have large uncertainties due to poor knowledge of the kaon coupling constants. As a result, it is yet to be demonstrated whether the kaon electromagnetic form factor can be extracted from exclusive K^+ electroproduction, as has been done recently at JLab for the π^+ case. The proposed measurement will for the first time acquire high quality L-T separated data above the resonance region, which is essential for a better understanding of the K^+ reaction mechanism. The results from the proposed measurement may also help to identify missing elements in existing calculations of the kaon production cross section. If these studies indicate K^+ pole dominance at low $-t$, then we would use these data to extract the K^+ charge form factor for $Q^2 > 0.35 \text{ GeV}^2$.

2. $1/Q^n$ Scaling Tests

Separated $p(e, e'K^+)\Lambda, \Sigma^0$ cross sections allow investigations of the transition from hadronic to partonic degrees of freedom in exclusive processes. Recent π^+ data from JLab suggest that the power law behavior expected from the hard scattering mechanism is reasonably consistent with the Q^2 -dependence of longitudinal cross section data. The Q^2 -dependence of the pion form factor is also consistent with the Q^2 scaling expectation already at values of $Q^2 > 1 \text{ GeV}^2$, even though the observed magnitude is larger than the hard QCD prediction. The latter may, for instance, be due to QCD factorization not being applicable in this regime or due to insufficient knowledge about additional soft contributions from the wave function in meson production. Since there is no single criterion for the applicability of factorization, tests of every necessary condition are needed. A direct comparison of the scaling properties of the K^+ separated cross sections would thus provide another important tool for the study of the onset of factorization in the transition from the hadronic to the partonic regime for Q^2 up to 5.5 GeV^2 , and provide a possibility to study effects related to SU(3). We propose a systematic measurement of the Q^2 dependence of the longitudinal and transverse cross sections at fixed $x_B=0.25, 0.40$ in charged kaon electroproduction. One may expect that the longitudinal cross section evolves towards Q^{-6} scaling in the hard scattering regime, and a significant longitudinal response may be indicative of the realization of the scaling expectation of the GPD formalism for charged kaon electroproduction. Transverse contributions are expected

to be suppressed by an additional factor of Q^{-2} .

4

We therefore propose to measure forward K^+ electroproduction by detecting the produced kaon in the SHMS in coincidence with the scattered electron in the HMS. We will extract the separated longitudinal and transverse cross sections via the Rosenbluth separation technique. Measurements in non-parallel kinematics will allow for simultaneous extraction of the interference terms and measurements of the $-t$ dependence of the K^+ cross section.

Because of the relatively low K^+ counting rates, the experimental uncertainties are expected to be statistics dominated and so it is more tolerant of higher systematic uncertainties than many other experiments already approved for the SHMS. This, coupled with the experiment's extensive use of 5-9 GeV beams, makes it an excellent early experiment candidate for the SHMS.

I. CONTRIBUTION TO THE HALL C 12 GEV UPGRADE

The co-spokespersons for this experiment plan to contribute to the implementation of the Hall C upgrade for 12 GeV in both manpower and materials.

Tanja Horn is supporting the SHMS optics design. She is working on the evaluation of the radiative heating of the SHMS horizontal bender magnet. This entails in part creating and maintaining a simulation of the magnet and the analysis of data obtained with a prototype. In addition, she is working with the design and engineering division on the implementation of spectrometer optics calculations to guide the design and construction of the SHMS, and in particular, the horizontal bender.

Garth Huber intends to apply to the Natural Sciences and Engineering Research Council of Canada (NSERC) for a Research Tools and Instrumentation grant (approximately \$100kUSD) in support of the SHMS Heavy Gas Čerenkov detector. The design studies are already in an advanced stage, and this application is expected to be submitted in October, 2009. Should these funds be granted by the Government of Canada, he intends to lead the construction efforts of this detector in collaboration with Hall C scientific and technical staff. In either event, the Regina group intends to provide manpower in support of the R&D, construction and commissioning of this detector.

Pete Markowitz will work on the SHMS commissioning, as well as the software and data acquisition upgrades. The SHMS will require verification of the optics and measurements of acceptance and detector efficiencies. He has previously worked on the Halls A and C spectrometer commissioning and software for Hall A analysis.

A. Scientific Motivation

By performing a measurement of separated $p(e, e' K^+) \Lambda, \Sigma^0$ cross sections, we have the unique opportunity to elucidate the reaction mechanism underlying strangeness production and the transition from hadronic to partonic degrees of freedom in exclusive processes.

1. Studies of the Kaon Electroproduction Mechanism above the Resonance Region

Despite many decades of effort, a comprehensive description of the reaction mechanism underlying strangeness production from a proton is still not available. This situation, compared to that of pion photoproduction, might be attributed to the experimental challenges encountered in kaon production. For instance, the kaon production cross section is smaller, and kaon PID is more challenging due to the short lifetime and separation of kaons from pion and proton backgrounds. As a result, the existing data have large uncertainties, and there are practically no data above the resonance region. In addition, poor knowledge of the relevant coupling constants adds to the complexity of the phenomenological investigations in this field.

L-T separations of exclusive K^+ production cross section above the resonance region are essential for a better understanding of both existing data and proposed measurements at Jefferson Lab. The separated results will, for instance, provide the foundation for a possible extraction of the K^+ form factor from electroproduction data. The challenges that need to be addressed are the quantification of the role of the kaon pole given that it is much further from the physical region than the pion pole, and that the K^+ longitudinal cross section may be sensitive to both the kaon charge form factor as well as a transition form factor between the kaon and an orbital excited state lying on the kaon Regge trajectory [1].

One of the main interests in the Q^2 dependence of kaon electroproduction is whether there is evidence for a large longitudinal cross section. This may be expected from analogy to the forward peak observed in charged pion production due to the pion pole. A large kaon exchange contribution, along with the dominance of the Λ coupling constant, would explain the small Λ/Σ^0 cross section ratio observed in electroproduction. However, it is not clear from the available data if there are significant enhancements due to the t channel exchange above the resonance region. An extrapolation of electroproduction data to the photoproduction point suggests that σ_L may indeed be large. This would be in conflict with the general expectation that the kaon pole, being farther away from the physical region, is of less consequence compared to the pion case. Measurements of kaon production over a wide kinematic range, and extending to small values of Q^2 , would address this issue.

As an example, in Figure 1 we show previous separated $K^+\Lambda$ and $K^+\Sigma^0$ cross section data from Hall C, taken at $W=1.84$ GeV, in the nucleon resonance region [2]. The data suggest that the contribution of transversely polarized photons is significant at $Q^2=2.0$ GeV 2 . This trend may

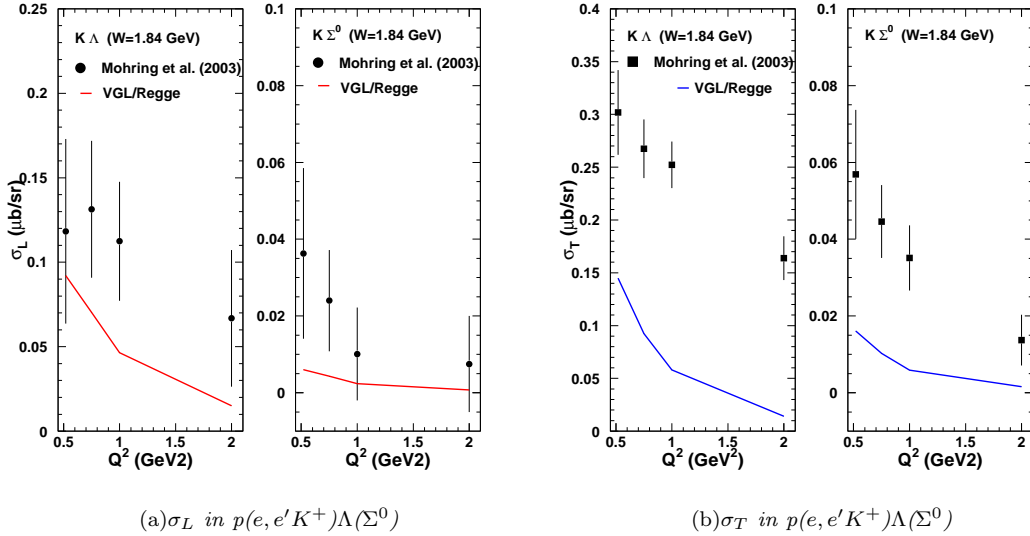


FIG. 1: The Q^2 dependence of the separated cross sections for electroproduction of kaons. The data are from JLab E93-018 [2]. The solid curves denote VGL Regge calculations with $\Lambda_K^2 = 1.5 \text{ GeV}^2$ and $\Lambda_{K^*}^2 = 1.5 \text{ GeV}^2$. Note that the data were taken at $W = 1.84 \text{ GeV}$, in the nucleon resonance region, where the VGL Regge model [1] is not expected to work particularly well.

be expected since the pole term contributing to σ_L decreases more rapidly with increasing distance from the pole, while σ_T is largely independent of it. However, a comparison of the data with the Regge model by Vanderhaeghen, Guidal, and Laget (VGL) [1, 3] raises some interesting questions.

We chose the comparison with the VGL Regge model as an example of a complete model of kaon production, because it has no adhoc parameters, and its validity has been established over a kinematic range in t and W for both pion and kaon photoproduction and electroproduction data. In this model, the pole-like propagators of Born term models are replaced with Regge propagators, and so the interaction is effectively described by the exchange of a family of particles with the same quantum numbers instead of the exchange of one particle. The K^+ version of the model incorporates both the K ($J = 0$) and the K^* ($J = 1$) trajectories, with free parameters Λ_{K,K^*} , the K, K^* trajectory cutoff parameters. Since the Regge model assumes a monopole form factor

$$F_K(Q^2) = [1 + Q^2/\Lambda_K^2]^{-1}, \quad (1)$$

Λ_K can be varied to obtain the best fit with the σ_L data. If the model successfully describes both the magnitude and the t -dependence of the data, F_K can be found for that Q^2 from substitution of Λ_K into the above equation.

In the case π^+ electroproduction, good agreement is obtained between the pion form factor mass scale obtained from a best fit to $p(e, e' \pi^+) n$ σ_L data ($\Lambda_\pi^2 \approx 0.5 \text{ GeV}^2$, $r_\pi^2 = 0.47 \text{ fm}^2$) [4] and the value measured by direct scattering of pions on atomic electrons at the CERN SPS (0.431 fm 2) [5]. This, along with the good description of the t -dependence of the σ_L data by the VGL

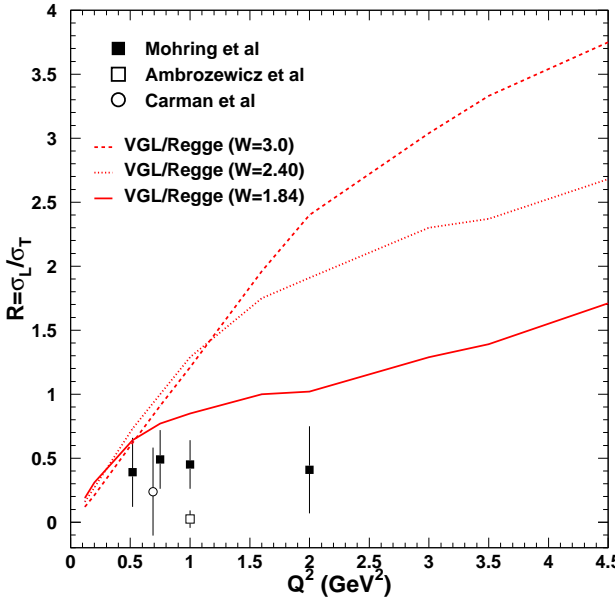


FIG. 2: *The ratio of longitudinal and transverse kaon electroproduction cross sections. All data points have been scaled to $W=1.84$ GeV. The curves denote predictions from the VGL Regge model for three different values of W . The data suggest that the L/T ratio is rather small, but the VGL Regge model suggests that the ratio has a strong dependence on W .*

Regge model, strongly indicate that at low $-t$ these data are dominated by the t -channel π^+ pole term and that a reliable value of the pion charge form factor can be extracted from the data using this model.

This is not the case for K^+ electroproduction. While at first sight a traditional Born model (with a $1/(t - m_K^2)$ standard Feynman propagator) seems to lead to a mass scale for the kaon electromagnetic form factor ($\Lambda_K^2 = 0.68$ GeV 2) compatible with the kaon charge radius, this model is unable to correctly reproduce the correct energy and t -dependences of the data [1]. Furthermore, it is unable to take into account the role of K^* exchange. Properly accounting for the exchange of higher spin particles is one of the major motivations of the VGL Regge model. In this model, the best fit value of the K trajectory cutoff mass ($\Lambda_K^2 = 1.5$ GeV 2 , $r_K^2 = 0.16$ fm 2) is much smaller than the value measured by direct scattering of kaons on atomic electrons (0.34 fm 2) [6]. VGL speculate that the discrepancy for the kaon case could be because the form factor used in this kind of model does not represent the properties of the kaon itself but rather the properties of the whole trajectory, which might be sensitive to transitions between the kaon and an orbital excited state lying on the kaon Regge trajectory [1]. If true, this would have to be kept in mind when trying to extract the kaon electromagnetic form factor from electroproduction σ_L data.

A likely alternate explanation could be that the $W = 1.84$ GeV value for these data are

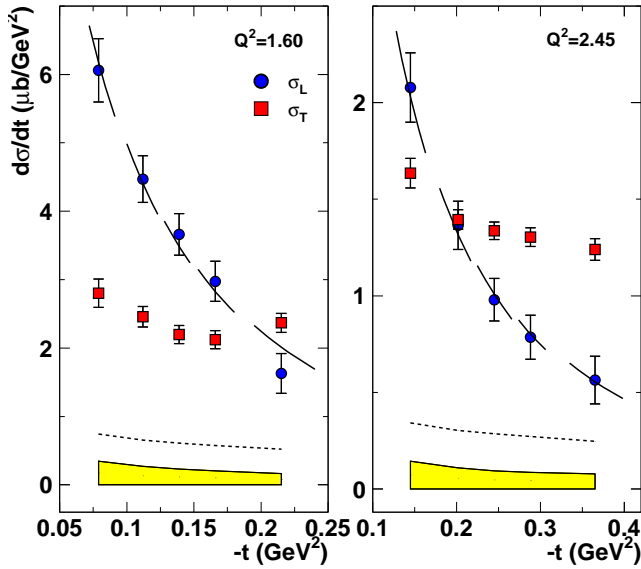


FIG. 3: The $-t$ dependence of the longitudinal and transverse π^+ cross sections. The data points are from the recently completed analysis of the E01-004 ($F_{\pi-2}$) experiment [4].

simply too low for the reliable application of the VGL Regge model. Indeed, figure 2 suggests a rather strong W dependence of the L/T ratio. Unfortunately, the only separated $p(e, e' K^+) \Lambda$ data in existence above the resonance region were taken at Cornell in the 1970's [7], and they suffer from very large statistical and systematic uncertainties. We propose to measure L-T separated cross sections for $W > 2.4$ GeV as a function both $-t$ and Q^2 , to investigate the K^+ reaction mechanism and determine whether it is feasible to extract the K^+ form factor from data of this type. Should we conclude that this extraction is feasible, this experiment would be the first determination of the K^+ form factor above the upper limit of the CERN SPS data.

These data may also shed light on a question raised by our recent $p(e, e' \pi^+) n$ L-T separations up to $Q^2 = 2.45$ GeV 2 , $W = 2.2$ GeV [4]. While the VGL Regge model provides an acceptable description of the σ_L data, it has consistently underestimated the magnitude of σ_T , for which the model seems to have limited predictive power. This is displayed in Figure 3. Similar discrepancies between σ_T data and the VGL Regge model have been observed in the π^0 channel [8]. Various improvements to the reaction mechanism in the model have recently been suggested [9]. A comparison of these models to high quality σ_T data for both the pion and the kaon would provide an important constraint for future improvements to the Regge model used for the extraction of the pion form factor.

One of the constraints in reaction mechanism tests underlying strangeness production is the $K^+ \Sigma^0 / K^+ \Lambda$ ratio [10]. The results from earlier experiments suggest that the ratio of longitudinal cross sections decreases slowly with increasing Q^2 . This was attributed to differences in the $g_{pK\Lambda}^2$

and $g_{pK\Sigma^0}^2$ coupling constants, assuming that σ_L is dominated by the t channel exchange diagram. However, it has been suggested that this model is not tenable [11] as it is inconsistent with the cross section at the photoproduction point. It is thus essential to test the electroproduction reaction mechanism, and in particular with data above the nucleon resonance region, since these do not contain this additional complication.

To address questions such as these, we propose to measure forward K^+ electroproduction by detecting the produced kaon in the SHMS, in coincidence with the scattered electron in the HMS. We will extract the separated longitudinal and transverse cross sections via the Rosenbluth separation technique. Measurements in non-parallel kinematics will allow for simultaneous extraction of the interference terms and measurements of the $-t$ dependence of the K^+ cross section.

2. Scaling of the Separated Cross Sections

The QCD-parton picture of the hadron predicts a separation of short-distance and long-distance physics at sufficiently high Q^2 . Measurements of inclusive processes, such as deep-inelastic scattering (DIS), confirm that in the limit of large Q^2 , at fixed values of x_B , such processes can be viewed as scattering from individual partons within the hadronic system. A similar separation (factorization) of scales may be expected to apply to hard exclusive scattering and allow the use of perturbative QCD (pQCD) concepts for exploring hadron structure.

One of the predictions of the factorization theorem is that in the large Q^2 limit, the dominant virtual photon polarization is longitudinal. The corresponding cross section scales to leading order like $\sigma_L \sim Q^{-6}$ at fixed x_B and $-t$, modulo higher order corrections [12]. The contribution of transversely polarized photons is suppressed by an additional power of $1/Q$ in the amplitude. In the Q^2 -scaling limit, pQCD describes the short distance process and Generalized Parton Distributions (GPDs) provide access to the non-perturbative physics. The dominance of the longitudinal amplitude by a factor of $1/Q$ is important because it contains information about the GPDs one would in fact like to extract.

Recent π^+ data from JLab indicate a $1/Q^6$ -scaling of the longitudinal cross section (σ_L) that is consistent with a hard scattering mechanism already at values of $Q^2 > 1$ GeV [13], but the transverse cross section (σ_T) does not show a corresponding $1/Q^8$ behavior. The Q^2 -dependence of the pion form factor is also consistent with the $1/Q^2$ scaling expectation for $Q^2 > 1$ GeV 2 , even though the observed magnitude is much larger than the hard QCD prediction (Fig. 4). The latter puzzle may, for instance, be due to QCD factorization not being applicable in this regime, or due to insufficient knowledge about additional soft contributions from the wave function in meson production. Results from recent analyses of the ρ^0 and ω [16–18] channels seem to support the former, while large angle Compton scattering data [19, 20] suggest that higher order corrections are dominant at currently available energies.

It would thus be of great interest to determine whether the scaling observed for σ_L and the

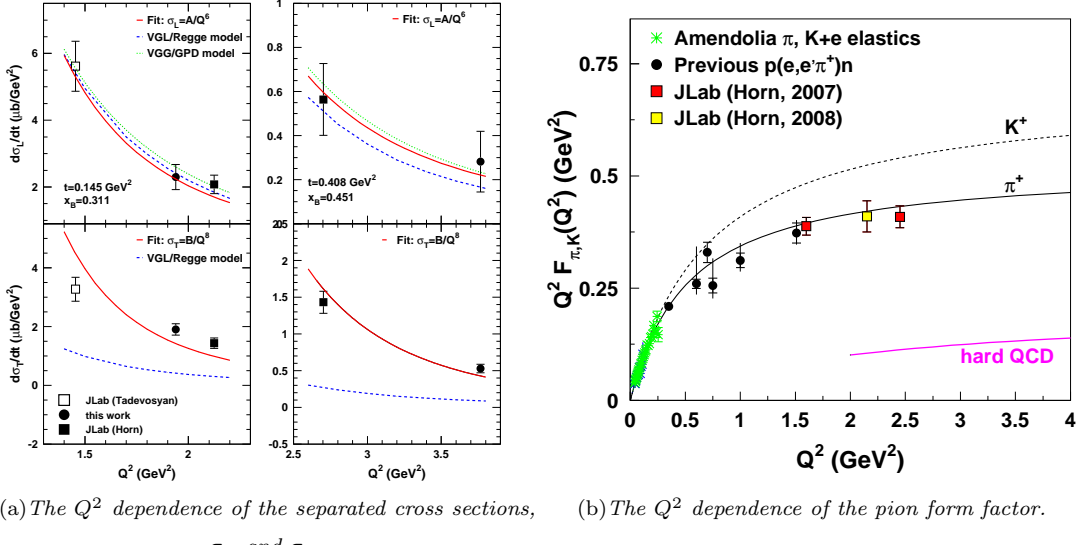


FIG. 4: The apparent scaling puzzle in pion electroproduction. The data are from [4, 13, 15]. These recent π^+ data from JLab indicate a Q^2 -scaling of the longitudinal cross section (σ_L) that is consistent with a hard scattering mechanism already at values of $Q^2 > 1 \text{ GeV}$ [13], but the transverse cross section (σ_T) does not show a corresponding behavior. The Q^2 -dependence of the pion form factor is also consistent with the Q^2 scaling expectation for $Q^2 > 1 \text{ GeV}^2$, even though the observed magnitude is larger than the hard QCD prediction.

pion form factor also manifests itself in other similar systems. The kaon, where one of the light quarks is replaced by a heavier strange one, makes a natural comparison. Analogous to the pion production reaction, one may thus expect to observe Q^{-6} scaling of σ_L at sufficiently high values of Q^2 . The threshold for the onset of factorization may be slightly higher due to the increased strange quark mass, and is expected to occur for values of $Q^2 > 5 \text{ GeV}^2$. SU(3) flavor symmetry relates the $p\Lambda$ GPDs to the usual GPDs in the proton, which may then allow for the extraction of information on quark transverse momentum distributions and angular momentum.

The size of transverse contributions to the forward kaon electroproduction cross section at moderate values of Q^2 , in particular in the Σ^0 channel, has been controversial for a long time, and the lack of L-T separated data above the resonance region complicates theoretical estimates. Looking at the s channel, it was found that for scattering followed by hadronization by vector gluons, the transverse-transverse interference term of the cross section is strictly zero [14]. However, in scattering by a transversely polarized photon followed by hadronization by a scalar gluon, it was found that σ_{TT} is not equal to zero. In this hard scattering limit, σ_T is expected to follow the Nachtmann prediction as a function of $-t$. A similar trend can be found in pion electroproduction data, where one measures the ratio of π^+ production off the proton to π^- production off the neutron. This ratio is expected to follow the Nachtmann prediction as $|t|$ increases. In the same limit, one would also expect the hard scattering condition $\sigma_L \gg \sigma_T$ to be valid.

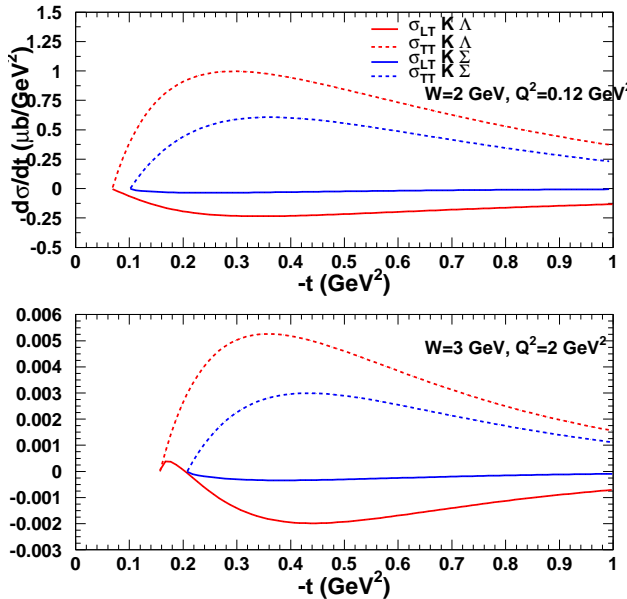


FIG. 5: The t dependence of the LT (red) and TT (blue) kaon electroproduction cross section interference terms as predicted by the VGL Regge model.

At higher Q^2 , kaon electroproduction probes the polarized quark GPDs \tilde{E} and \tilde{H} , which by SU(3) flavor symmetry can be related to the strangeness polarization in the nucleon. Analogous to π^+ production, in the limit $-t \rightarrow m_K^2$ the K^+ production amplitude contains a “pole term” governed by the kaon form factor, which in the region $x_B > 0.1$ at high Q^2 is governed by the hard scattering mechanism closely related to high- Q^2 kaon production. Although it is known that the K^+ pole term in the $p \rightarrow \Lambda$ GPD is less prominent because the pole at $-t=m_K^2$ is further removed from the physical region ($t < t_{min} < 0$), our understanding of the reaction mechanism in kaon electroproduction is far from clear.

Measurements of the the Q^2 dependence in the $Q^2=1\text{-}6 \text{ GeV}^2$ region would thus be a great leap forward in our understanding of meson electroproduction, even if the onset of scaling only occurs at very high values of Q^2 .

It has been suggested that additional information about QCD factorization may be obtained through the interference terms [21]. In the hard scattering limit, these terms are expected to scale as Q^{-7} and Q^{-8} for LT and TT respectively. Since we will perform a full deconvolution of all four response functions, we will test these additional expectations as well. Figure 5 shows the interference terms in kaon production as predicted by the VGL Regge model.

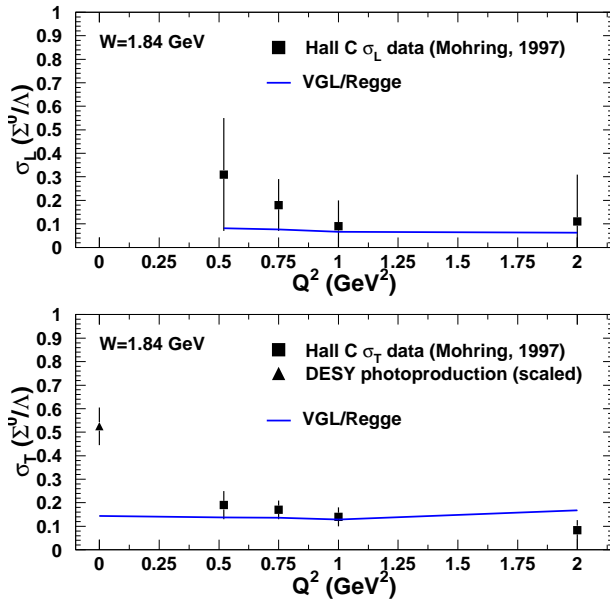


FIG. 6: The Q^2 dependence of the ratio of longitudinal and transverse cross sections for kaon electroproduction with Σ^0 and Λ final states. The data are from Ref. [2] and were taken in the resonance region at $W=1.84$ GeV. The curves denotes VGL model calculations for the Σ^0/Λ final state cross section ratios for these kinematics.

3. Previous Data and Analyses

Although precise meson production measurements have recently become available at accelerators like Jefferson Lab, kaon electroproduction data above the resonance region remains sparse. The early, unseparated data from CEA [22] and Cornell [7, 23] cover values of $Q^2 < 1.2$ GeV 2 (< 2 GeV 2 at Cornell) and values of W between 1.8 and 2.67 GeV. The results from these experiments suggest the dominance of the Λ over the Σ^0 channel. However, no explicit separation of the response functions was performed. The first attempt of an L-T separation was made at Cornell for values of Q^2 between 1.19 and 3.38 GeV 2 and values of W ranging between 2.14 and 2.56 GeV [7]. Due to statistical limitations, data had to be combined for different targets and running periods, and the longitudinal cross section was isolated by subtracting a model of the transverse contribution from the unseparated cross sections. The reported ratio of σ_L/σ_T suggest (with large uncertainties) a dominant σ_L in the Λ channel, but not the Σ^0 channel. Kaon electroproduction data were also obtained at DESY for a value of W of 2.2 GeV and for values of Q^2 ranging between 0.06 and 1.35 GeV 2 [24]. The large acceptance detector in this experiment allowed for the determination of the interference terms σ_{LT} and σ_{TT} . However, σ_L and σ_T could not be separated. The data suggest interference terms consistent with zero, but with relatively large uncertainties.

The availability of the high-intensity, continuous electron beams and well-understood magnetic spectrometers at Jefferson Lab made it possible to determine kaon electroproduction cross sections with high precision. In 1997, high-precision kaon electroproduction data for values of Q^2 between 0.52 and 2.00 GeV^2 were acquired at Jefferson Lab in Hall C at a value of the invariant mass of the photon-nucleon system of $W=1.84 \text{ GeV}$ [2]. These data suggest a ratio $\sigma_L/\sigma_T \approx 0.4$ for both the Λ and Σ^0 channels in these kinematics. As illustrated in Figure 6, the ratio of the separated Λ and Σ^0 cross sections indicate a mild decrease with increasing Q^2 . This trend is not consistent with earlier electroproduction data from DESY taken at a higher W and over a wider range of Q^2 and W . Discrepancies between data and model predictions could be due to significant resonance contributions, especially in the Σ^0 channel in this kinematic regime.

Kaon electroproduction data were also obtained in Hall A at Jefferson Lab for values of W from 1.8 to 2.14 GeV for values of Q^2 of 1.9 and 2.35 GeV^2 [25]. Limitations in the incident beam energy precluded the acquisition of data above the resonance region. The Hall A PID, spectrometer minimum angle of 12.5° , and spectrometer momentum range also limited the maximum Q^2 and W to values well below that of the current proposal. The experimental technique used was similar to that of the Hall C measurement, although the $-t$ dependence of the cross section was obtained through a scan in the invariant mass W rather than in the angle, θ_K , with respect to the q -vector (see Sec.II). A ratio of $\sigma_L/\sigma_T \sim 0.5$ was observed [26]. The t -dependence of the σ_L cross section was found to be rather flat, as would be expected if the kaon pole was dominant. [The pion pole term, with a smaller mass, gives a sharper rise while the kaon pole term is both broader and lower.] The production mechanism is not determined above the resonance region and it has not yet been shown that the kaon form factor can be extracted from the measurements. There is also no data about Q^2 -scaling such as this proposal will measure.

The most comprehensive photoproduction data were acquired with the CLAS in Hall B [27, 28]. Although the smallest angle reported is $\cos\theta_{CM} = 0.9$, or 25° , the photoproduction data exhibit the same forward peaking of the cross section as the electroproduction data. This is interpreted as t -channel forward angle dominance. On the other hand, above the third resonance region $W > 1.9 \text{ GeV}$, the W -dependence was observed to be flat at forward angles.

Kaon electroproduction data acquired with the CLAS in Hall B [29, 30] exploited the recoil polarization technique in which one measures the polarization transfer from the virtual photon to the produced hyperon for $Q^2 = 0.3 - 1.5 \text{ GeV}^2$ and $W=1.6-2.15 \text{ GeV}$. The σ_L/σ_T ratio, extracted at $\theta_K^*=0^\circ$, was smaller, but consistent with the earlier Hall C result. A more recent analysis of kaon data [31] presented a full separation of the cross section components for the Λ and Σ^0 channels over a momentum transfer range of $0.5 < Q^2 < 2.8 \text{ GeV}^2$ and a center of mass energy range of $1.6 < W < 2.4 \text{ GeV}$. The data are in good agreement with the electroproduction data from Hall C at Jefferson Lab [2], but are inconsistent with the photoproduction result.

Summarizing, both the photoproduction and the electroproduction of $K^+\Lambda$ pairs are t -channel dominated at forward angles. The cross section is forward peaked, the fifth re-

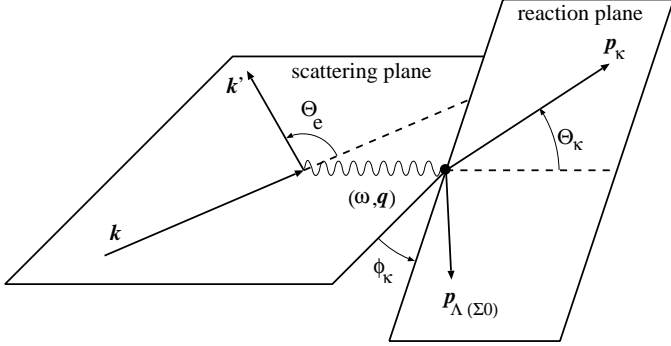


FIG. 7: Kinematics of the $p(e, e' K^+) \Lambda(\Sigma^0)$ reaction.

sponse function is small, consistent with only a single channel dominating the response, and the W -dependence and forward angle polarizations are smooth. [Although there is interesting structure at more backward angles and lower W .] The ratio $\sigma_L/\sigma_T \approx 0.4$ and the Q^2 dependence are broadly consistent with a monopole fall-off. The t -channel dominance is necessary for experiments to measure Q^2 scaling, the kaon form factor, or partonic degrees of freedom.

On the other hand, both photoproduction and electroproduction of $K^+\Sigma^0$ pairs shows s -channel dominance. The cross sections are not forward peaked, but peak around 90° . The W -dependence is not as smooth (especially away from the forward angles), and the polarizations exhibit more structure. The difference from Λ production is not understood.

II. EXPERIMENTAL METHOD

In this experiment we will measure separated cross sections for the $p(e, e' K^+) \Lambda(\Sigma^0)$ reaction using the Rosenbluth separation technique.

The kinematics of the $p(e, e' K^+) \Lambda(\Sigma^0)$ reaction are illustrated in Figure 7. The incident electron with four momentum $k=(\epsilon_k, \mathbf{k})$ scatters through an angle θ_e to a final four momentum $q=(\omega, \mathbf{q})$. The electron scattering plane is defined by the three momenta \mathbf{k} and \mathbf{k}' , and also includes the exchanged virtual photon three momentum transfer \mathbf{q} . The virtual photon is absorbed by the target proton and a kaon is emitted with four-momentum $p'=(E(p'), \mathbf{p})$, where \mathbf{p} is oriented relative to the scattering plane by a polar angle θ_K and an azimuthal angle ϕ_K .

The unpolarized pion electroproduction cross section can be written as the product of a virtual photon flux factor and a virtual photon cross section,

$$\frac{d^5\sigma}{d\Omega_e dE'_e d\Omega_K} = J(t, \phi \rightarrow \Omega_K) \Gamma_v \frac{d^2\sigma}{dt d\phi}, \quad (2)$$

where $J(t, \phi \rightarrow \Omega_K)$ is the Jacobian of the transformation from $dt d\phi$ to $d\Omega_K$, ϕ is the azimuthal angle between the scattering and the reaction plane, and $\Gamma_v = \frac{\alpha}{2\pi^2} \frac{E'_e}{E_e} \frac{1}{Q^2} \frac{1}{1-\epsilon} \frac{W^2-M^2}{2M}$ is the virtual photon flux factor. The virtual photon cross section can be expressed in terms of contributions

from transversely and longitudinally polarized photons,

$$2\pi \frac{d^2\sigma}{dtd\phi} = \frac{d\sigma_T}{dt} + \epsilon \frac{d\sigma_L}{dt} + \sqrt{2\epsilon(1+\epsilon)} \frac{d\sigma_{LT}}{dt} \cos\phi + \epsilon \frac{d\sigma_{TT}}{dt} \cos 2\phi. \quad (3)$$

Here, $\epsilon = \left(1 + 2\frac{|\mathbf{q}^2|}{Q^2} \tan^2 \frac{\theta}{2}\right)^{-1}$ is the virtual photon polarization, where \mathbf{q}^2 is the square of the three-momentum transferred to the nucleon and θ is the electron scattering angle. The interference terms, σ_{LT} and σ_{TT} , can be eliminated by averaging over ϕ_K , and the longitudinal and transverse cross sections can be separated by measuring the cross section at two or more values of ϵ .

In parallel kinematics, it is not possible to measure the $-t$ dependence of the cross section at fixed W , Q^2 , since these three variables are not independent. In order to measure the $-t$ dependence, one must thus vary θ_K away from parallel kinematics. In this case, σ_{LT} and σ_{TT} also contribute and additional data are required for a complete separation. A measurement of the ϕ_K dependence of the data at fixed W , Q^2 , $-t$ is therefore required.

A. Proposed Kinematics

We propose to examine the Q^2 dependence of the cross section at several x_B points, and at fixed values of $-t$ that are small relative to Q^2 . Figure 8 shows the accessible Q^2 - x_B phase space for this experiment. The higher energies available at a 12 GeV JLab allow for access to a significantly larger range in Q^2 for values of W above the resonance region compared to what one could achieve at the 6 GeV JLab. The access to higher values of W is important because it provides the first K^+ data which allow for a reliable interpretation of, for instance, the $-t$ and Q^2 dependences of σ_L . The low values of $-t$ would also be favorable for the possible extraction of the kaon form factor if warranted by the data. The proposed kinematics also allow for a scan of the Q^2 dependence of the cross section at constant x_B while staying above the resonance region. Our proposed measurement will provide the first data in this region.

Table I lists the kinematic settings for this experiment. Coincidence measurements would be made between kaons in the SHMS and electrons in the HMS. The SHMS will detect kaons in near-parallel kinematics (θ_K near zero), which will allow for the separation of the individual cross section components. We have assumed that the SHMS can be set to angles ranging between 5.5° and 30° , and that the minimum opening angle between the spectrometers can be no less than 18.0° when the HMS is located at 10.5° . To determine σ_L and σ_T from the data, a minimum of two beam energies is required. To minimize the amplification in the systematic uncertainty, the ϵ settings have been chosen to span $\Delta\epsilon \gtrsim 0.20$ where possible.

In order to do a full separation of the L, T, LT and TT terms over a wide $-t$ range, data will also be acquired to the left and right of \vec{q} . Figure 9 shows simulated $x_B=0.40$ SHMS+HMS data, where θ_K was varied by $\pm 3^\circ$ from the near-parallel kinematics. The ϕ_K coverage allows σ_{LT} and σ_{TT} to be obtained from the measured ϕ_K dependence of the cross section.

Figure 10 shows the range of Q^2 and W acceptance at $x_B=0.25$. At the high ϵ setting,

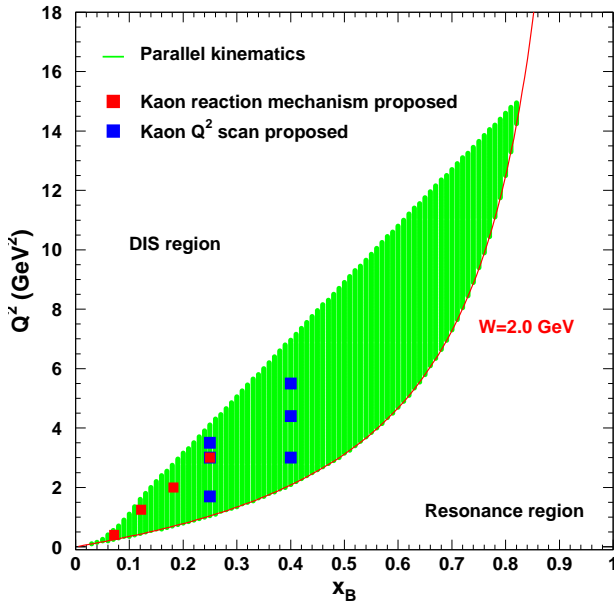


FIG. 8: Q^2 versus x_B phase space available for L-T separations in Hall C at 11 GeV using the SHMS+HMS combination. We propose to measure the Q^2 dependence of the longitudinal cross section at $x_B=0.25$ and $x_B=0.40$, and the t dependence of the longitudinal cross section for values of $Q^2=0.40$ to 3.00 GeV 2 . The kinematic reach is limited from below by the requirement on W being above the resonance region and from above by the requirement to maintain a separation of $\Delta\epsilon \gtrsim 0.20$.

the acceptance in W and Q^2 is generally larger than for the low ϵ setting. To reduce systematic uncertainties, cuts will be placed on the data to equalize the Q^2 - W coverage at high and low ϵ .

We have included three beam energies at $Q^2=2.0$ GeV 2 to provide a consistency check in the determination of σ_L and σ_T . Our remaining Q^2 settings are dominated by counting statistics, and additional beam energies would require a significantly larger amount of beam time to significantly improve the overall uncertainty. We thus propose only 2 ϵ settings for these kinematics. A more detailed discussion of the benefit of multiple ϵ settings also considering the systematic and statistical uncertainty can be found in Appendix A.

The scan of the $-t$ dependence at $Q^2=0.40$, 1.25 , 2.00 and 3.00 GeV 2 will provide L-T separated data, from which the contributions of σ_L and σ_T to the Λ and Σ^0 final states can be determined. This would provide important information about the role of K and K^* exchange contributions (in the t -channel). If the K pole contribution at low $-t$ for the $K^+\Lambda$ channel dominates σ_L , these data could be used to extract the kaon form factor analogous to the π^+ case [32]. A comparison of the $Q^2=0.40$ GeV 2 data with the elastic form factor data at CERN will allow for a check of the overall normalization of the form factor. The data at higher Q^2 could provide the first extraction of the form factor at higher Q^2 above the resonance region. Keeping

TABLE I: *Kinematic settings for the $p(e, e' K^+) \Lambda(\Sigma^0)$ measurement. The scattered electron will be detected in the HMS and the K^+ in the SHMS. The kinematics have been optimized to allow the data point at $Q^2=3.0$ GeV 2 , $W=3.14$ GeV to be used for both the reaction mechanism and the scaling studies. This reduces the required beam time and also improves the statistical uncertainty for the scaling study (which has generally lower statistics).*

W (GeV)	Q^2 (GeV 2)	E_e (GeV)	E'_e (GeV)	θ_e (deg)	ϵ	p_K (GeV)	θ_K (deg)	$-t_{min}$ (GeV/c) 2	x	R
Intermediate Q^2 for reaction mechanism and form factor Q^2 dependence										
2.45	0.40	3.80	0.857	20.17	0.411	2.669	5.64	0.064	0.072	0.55
2.45	0.40	5.00	2.057	11.31	0.692	2.669	7.71	0.064	0.072	0.55
3.14	1.25	7.40	1.949	16.93	0.477	5.189	5.85	0.084	0.122	1.19
3.14	1.25	9.30	3.849	10.72	0.696	5.189	7.39	0.084	0.122	1.19
3.14	2.00	7.50	1.649	23.19	0.396	5.561	6.20	0.138	0.182	2.37
3.14	2.00	8.80	2.949	15.96	0.584	5.561	7.74	0.138	0.182	2.37
3.14	2.00	10.90	5.049	10.94	0.751	5.561	9.16	0.138	0.182	2.37
3.14	3.00	8.20	1.816	25.93	0.393	6.053	6.90	0.219	0.250	3.15
3.14	3.00	10.90	4.516	14.18	0.689	6.053	9.63	0.219	0.250	3.15
Scaling study at fixed $x=0.25$, $-t=0.2$										
2.45	1.70	5.60	1.965	22.67	0.587	3.277	11.31	0.239	0.249	1.87
2.45	1.70	8.80	5.165	11.10	0.858	3.277	14.92	0.239	0.249	1.87
3.37	3.50	9.30	1.852	26.05	0.357	7.122	6.08	0.215	0.250	3.75
3.37	3.50	10.90	3.452	17.54	0.555	7.122	7.79	0.215	0.250	3.75
Scaling study at fixed $x=0.40$, $-t=0.5$										
2.32	3.00	6.60	2.602	24.12	0.634	3.486	14.13	0.531	0.400	2.23
2.32	3.00	10.90	6.902	11.46	0.887	3.486	18.35	0.531	0.400	2.23
2.74	4.40	8.20	2.324	27.80	0.480	5.389	10.00	0.507	0.400	3.31
2.74	4.40	10.90	5.024	16.30	0.734	5.389	13.06	0.507	0.400	3.31
3.02	5.50	9.30	1.978	31.73	0.366	6.842	7.78	0.503	0.400	3.90
3.02	5.50	10.90	3.578	21.64	0.560	6.842	9.88	0.503	0.400	3.90

the low $-t$ constraint in mind, we have chosen kinematics with values of $-t$ that are less than three times the pole value.

The Q^2 scans at fixed values of $x_B=0.25$ and $x_B=0.40$ accesses the regime between 1.0-5.5 GeV 2 for the first time above the resonance region and will provide reliable L-T separated data for investigations for the onset of $1/Q^n$ scaling in strange systems. Since the measurement at $x_B=0.25$ is at relatively low Q^2 , these data are acquired relatively quickly and do not contribute greatly to the total beam time request. One of the goals of the proposed measurement is to extend our knowledge of the relative longitudinal and transverse contributions to the cross section to the

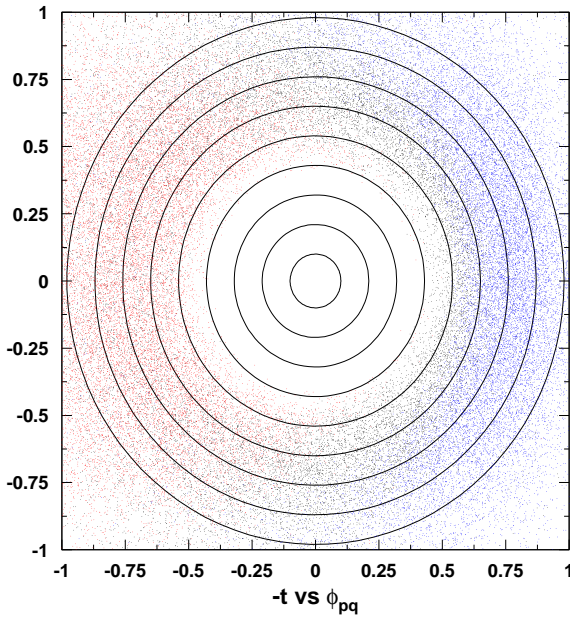


FIG. 9: Simulated $-t$ (radial coordinate) versus the azimuthal angle ϕ distributions for the proposed measurement using HMS+SHMS at $x_B=0.40$ and $Q^2=5.5 \text{ GeV}^2$. Each radial division corresponds to $-t = 0.10 \text{ GeV}^2$. The colors denote the kinematic points with the SHMS set at zero (black), $+3^\circ$ (blue), and -3° (red) with respect to the q -vector.

largest possible Q^2 . Given the constraint imposed by the requirement to keep $-t \ll 1 \text{ GeV}^2$, combined with the maximum available beam energy of the upgraded CEBAF and the kinematic reach of the SHMS+HMS configuration in Hall C, the maximum Q^2 is near 10 GeV^2 . At this point, $\Delta\epsilon$ is kinematically restricted. We have chosen to limit the maximum Q^2 to 5.5 GeV^2 as the ratio $R=\sigma_L/\sigma_T$ is effectively unknown, and the projected ratio based on previous kaon production data predict a rapid increase of the uncertainties at higher values of Q^2 . However, it should be emphasized that the run-plan requires only minor adjustments to reach a value of $Q^2=8 \text{ GeV}^2$, should new data indicate that the uncertainties would be acceptable.

The Q^2 coverage for the proposed measurement is a factor of three larger than what one could achieve with a 6 GeV configuration at much smaller values of $-t$ at larger W . This facilitates the determination of the Q^2 dependence even if the L/T ratios turn out to be less favorable than predicted by available models.

A high luminosity spectrometer system like the SHMS+HMS combination in Hall C is well suited for these measurements. The magnetic spectrometers benefit from relatively small point-to-point uncertainties, which are crucial for meaningful L-T separations. In particular, the optical properties and the acceptance of the HMS have been studied extensively and are well understood in the kinematic range between 0.5 and 5 GeV, as evidenced by more than 200 L-T

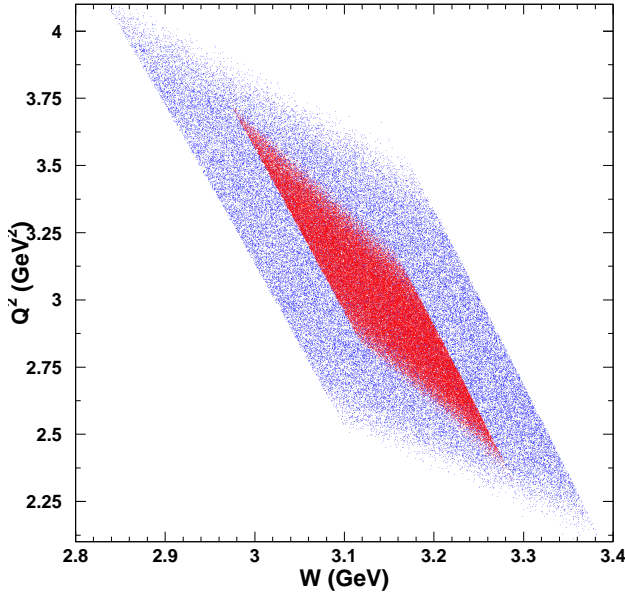


FIG. 10: Simulated Q^2 versus W coverage for the proposed measurement at $x_B=0.25$. The red data points correspond to the low and the blue data points to the high ϵ settings.

separations (~ 1000 kinematics) [33]. The position of the elastic peak has been shown to be stable to better than 1 MeV, and the precision rail system and rigid pivot connection have provided reproducible spectrometer pointing for more than six years. The main properties of the HMS have been incorporated into the design of the SHMS, and the measurements proposed here are expected to benefit from relatively small point-to-point uncertainties. In Hall C, previous kaon production coincidence experiments have achieved uncorrelated systematic uncertainties of 2.4 to 4.0%, mainly limited by the knowledge of the SOS acceptance [2].

Since E93-018 was one of the first experiments carried out in Hall C, the systematic uncertainties represent a worst case scenario. In general, the systematic uncertainty improves over time, as our knowledge about spectrometers and their acceptance builds up. The experiment proposed here is largely limited by counting statistics, and is more tolerant to systematic uncertainties than other approved SHMS experiments. It could thus take a similar early place in the cue of experiments after the 12 GeV upgrade is completed. In this early running scenario, although the projected systematic uncertainty for the proposed measurement would be larger than the other approved SHMS experiments, it would still compare favorably with the earlier Hall C HMS+SOS experiment.

A large acceptance device like CLAS12 is well suited for measuring pseudoscalar meson electroproduction over a large range of $-t$ and x_B . Although the large CLAS12 azimuthal coverage allows for a good determination of the interference terms, the main constraint remains the error

amplification in the extraction of the longitudinal and transverse components. In addition, the proposed kinematics would have significantly lower rates if run there, due to the lower Hall B luminosity. The use of the SHMS and HMS in Hall C is proposed here as their characteristics best address the experimental requirements, and the existing knowledge of the properties of the HMS is expected to allow for a well understood isolation of the longitudinal and transverse cross sections on the order of fifty days.

B. Particle Identification

For this experiment, the SHMS will be configured for kaon detection and the HMS for electron detection. Hadron identification in the SHMS is primarily done with coincidence time cuts. At higher momenta, time of flight within the SHMS detector stack will be unable to provide adequate species separation. The SHMS will thus be equipped with a series of Čerenkov detectors to provide additional methods to distinguish pions from protons and kaons, and improve the real-to-random signal.

π^+/K^+ separation will be provided by the heavy gas Čerenkov for $p_{SHMS} > 3.4 \text{ GeV}/c$. π^+/K^+ discrimination power is momentum dependent, varying from 100:1 at 3.4 GeV/c to $10^4:1$ at 7 GeV/c [34], so particle identification should not be a problem in this region. However, care has to be taken in the design and construction of this detector so that the design goals are met.

Reliable K^+/p separation above 3 GeV/c requires the construction of an aerogel Čerenkov detector. To span the range of SHMS momenta in this experiment (2.6 to 7.1 GeV/c), four different sets of aerogel will be needed. Details on a possible configuration for the aerogel detector that should provide at least 300:1 K^+/p separation are given in Appendix B. To optimize the efficiency, we assume that two aerogel detectors can be installed simultaneously in the SHMS detector stack.

C. Backgrounds

Singles rates from (e, K^+) and (e, p) can result in accidental coincidences which are a source of background for the measurement. The singles rates into both spectrometers were estimated and are summarized in Table II. For the electron rates, the QFS program by O'Connell and Lightbody [35] was used, while the hadron rates were estimated using a fit to experimental pion, kaon, and nucleon photoproduction at higher energies [36]. The projected singles rates are well below the anticipated capability of the detector packages, which we expect to be constructed to accommodate multi-MHz singles rates. The detector combination of aerogel and heavy gas Čerenkov is expected to provide good particle identification over the momentum range of the proposed measurement.

The π^+ singles rates are dominant for the proposed kinematics and good K^+ identification will be required. While pions that propagate to the SHMS detector hut can be discriminated using

TABLE II: *Projected SHMS and HMS rates for a 8-cm LH2 target, except for the lowest Q^2 setting where a 4-cm LH2 target was assumed. The accidental coincidence rates assume a resolving time of 40 ns, a 300:1 π^+ and p , and 25:1 π^- and K^- rejection, and correspond to the online rates. After offline cuts are applied, the accidental coincidences will be effectively eliminated.*

Q^2 (GeV 2)	ϵ	R(π^+) (kHz)	R(K^+) (kHz)	R(p) (kHz)	R(π^-) (kHz)	R(K^-) (kHz)	R(e^-) (kHz)	R(acc) (Hz)	R(real) (Hz)
0.40	0.411	1360	179	269	996	18	45	0.02	0.03
0.40	0.692	1615	247	365	360	11	411	0.02	0.04
1.25	0.477	435	145	100	203	10	43	0.3	0.04
1.25	0.696	409	136	106	62	5	239	1.3	0.05
2.00	0.396	220	87	61	109	5	11	0.05	0.01
2.00	0.751	170	67	47	12	1	27	0.5	0.02
3.00	0.393	105	48	35	36	2	6	0.02	0.0068
3.00	0.689	51	22	20	46	0.5	55	0.05	0.0098
1.70	0.587	235	61	102	32	1	27	0.07	0.01
1.70	0.858	140	38	81	14	0.3	367	0.6	0.02
3.50	0.357	83	45	27	35	2	4	0.0099	0.0049
3.50	0.555	48	24	17	9	0.8	2	0.0023	0.0059
3.00	0.634	72	22	44	3	0.1	14	0.01	0.02
3.00	0.887	28	9	24	0.6	0.02	202	0.07	0.03
4.40	0.480	37	16	18	3.1	0.1	4	0.003	0.006
4.40	0.734	12	5	7	0.4	0.03	28	0.0056	0.0085
5.50	0.366	31	17	13	4.4	0.2	1	0.0008	0.0023
5.50	0.560	12	6	6	0.8	0.07	5	0.0012	0.0027

the Čerenkov detector, a fraction of pions produced may decay. A significant fraction of these decay products may also propagate to the SHMS focal plane and cannot be eliminated by the Čerenkov detector. Those resulting from pion singles events will appear as random coincidences and will be subtracted away.

Projected rates for the HMS are relatively low and are well within the operating parameters of previous HMS experiments. In this experiment, we will reject π^- in the HMS at the hardware level. The electron will be identified using the lead-glass calorimeter in combination with the gas Čerenkov. On the trigger level, this translates to the logical OR of the high threshold preshower and gas Čerenkov signals combined with signals from both scintillator planes. Pion rejection rates of 25:1 may be achieved without significant inefficiency. The trigger efficiency may be monitored using a prescaled sample of pions. Previous experiments in Hall C have shown that after offline cuts on calorimeter, Čerenkov, and coincidence time, the π^- contamination is negligible.

In calculating the accidental coincidence rates, a 300:1 pion and proton rejection was as-

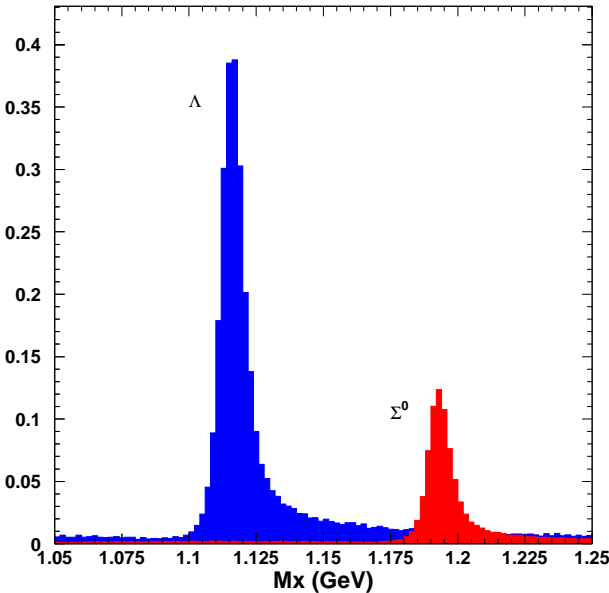


FIG. 11: *Simulated missing mass spectrum for $Q^2 = 2.0 \text{ GeV}^2$. The spectra for the other kinematic settings proposed here are similar.*

sumed in the trigger rate. The online π^- rejection rate was assumed to be 25:1. The online coincidence resolving time was taken to be 40 ns. For all settings, the resulting online real+random rates are well below the expected capability of the HMS+SHMS data acquisition system. Offline, where the resolving time is expected to be no worse than 2 ns, the accidental coincidence rates are not a significant source of background. Placing cuts on the missing mass will reduce the accidental background to just a few percent of the real coincidence rate.

The unobserved exclusive final state will be identified via the missing mass, which is reconstructed from the final electron and proton four-momenta. Cutting on the missing mass will reduce both random coincidences and background from events with larger inelasticity than $p(e, e' K^+) \Lambda(\Sigma^0)$. The missing mass acceptance is illustrated in Figure 11. The missing mass resolution is $\sim 30 \text{ MeV}$ at the high and low Q^2 settings and should be more than adequate for separating the exclusive final states and from each other.

To separate the $K^+ \Sigma^0$ final state, one also has to subtract the contribution from the Λ tail. The shape is largely dominated by radiative effects, but contributions from events that pass through the collimator may contribute as well. The latter will be included in the analysis via Monte Carlo techniques analogous to the procedure described in [37]. Based on previous kaon electroproduction data, we estimate the total effect of these contributions to be 1/10 of the size of the tail [26].

We have chosen a liquid hydrogen target with a length of 8 cm, except for the lowest Q^2

settings where a length of 4 cm was assumed. This means that the target end windows will be in the acceptance of both spectrometers in all configurations and background subtractions are necessary. Background events from the target end windows will be measured using “empty” target data. The Hall C empty target consists of two thin Aluminum pieces separated by a length equivalent to the cryogenic target length. However, the empty target is thicker by a factor of approximately ten relative to the target cell walls. The thicker target allows for a more rapid accumulation of counts for this background measurement. Assuming a maximum current of $30\mu\text{A}$ and $90\mu\text{A}$ for the empty and cryo targets, respectively, results in a background measurement faster by a factor of 3. Based on previous measurements in Hall C [37], we estimate the surviving window background for $p(e, e'K^+)\Lambda(\Sigma^0)$ to be on the order of 1% for a 8-cm target.

D. Systematic Uncertainties

The estimated systematic uncertainties are listed in Table III. These are based on previous experience with the HMS+SOS in Hall C. Assuming that thorough sieve optics measurements are performed in the first year of SHMS operation, we expect these systematic uncertainties to be reasonably achievable. In fact, in comparison to recent coincidence measurements with the HMS+SOS, we expect some improvements in the contributions to the systematic uncertainty. For example, the HMS acceptance is much flatter than the SOS acceptance and will not be affected significantly by magnetic field saturation.

Compared to previous experiments, the kaon momentum will be higher, and we expect the corresponding absorption correction to be smaller. The SHMS flight path is longer by about a factor of two compared to the SOS. The higher K^+ momentum, combined with the slightly longer SHMS flight path, will approximately balance the kaon decay correction. In comparison with previous SOS experiments, we expect that the correction and the corresponding systematic uncertainty to be similar. In comparison with the HRS experiments in Hall A, we expect an improvement of a factor of two since the HRSs have a longer flight path than the SHMS. The higher kaon momentum will also result in a smaller kaon absorption correction relative to previous HMS+SOS and HRS experiments.

The overall systematic uncertainties for K^+ detection in the SHMS are expected to be comparable to the systematic uncertainties characteristic of the HRS.

III. PROJECTED ERROR AND TIME ESTIMATE

In preparing the count rate estimate, we assume the following: 8-cm liquid hydrogen target thickness and $90\mu\text{A}$ electron beam current (4-cm target length and $35\mu\text{A}$ current for the lowest Q^2 setting), SHMS solid angle and momentum bite of 3.5 msr and 15%, and HMS solid angle and momentum bite of 5.9 msr and 8%. The dominant parameters in the beam time estimate are the

TABLE III: *Estimated systematic uncertainties for the K^+ unseparated cross section based on previous Hall C experience. The uncorrelated errors between the high and low ϵ settings are listed in the first and second column. The point-to-point uncertainties are amplified by $1/\Delta\epsilon$ in the L-T separation. The t-correlated uncertainties are also amplified, while the scale uncertainties propagate directly into the separated cross sections. The estimate for the radiative correction systematic uncertainty is only for the $K^+\Lambda$ channel. The fourth column gives the expected systematic uncertainty if the proposed measurement ran as one of the early experiments, and the last column lists the corresponding values for a later running time.*

Source	pt-to-pt	t-correlated	scale (earlier)	scale (later)
Acceptance	0.4	0.4	2.0	1.0
PID		0.4	1.0	0.5
Coincidence Blocking		0.2		
Tracking efficiency	0.1	0.1	1.5	1.5
Charge		0.2	0.5	0.5
Target thickness		0.2	0.8	0.8
Kinematics	0.4	1.0		
Kaon Absorption		0.5	0.5	0.5
Kaon Decay		1.0	3.0	3.0
Radiative Corrections	0.1	0.4	2.0	2.0
Monte Carlo Model	0.2	1.0	0.5	0.5
Total	0.6	2.0	4.7	4.2

ratio of the longitudinal to transverse cross sections, $R = \sigma_L/\sigma_T$ and the value of $\Delta\epsilon$ between the kinematic settings.

Two measurements at fixed Q^2 , W , $-t$ and different values of ϵ are required to determine σ_L . Letting $\sigma_1 = \sigma_T + \epsilon_1 \sigma_L$ and $\sigma_2 = \sigma_T + \epsilon_2 \sigma_L$ then

$$\sigma_L = \frac{1}{\epsilon_1 - \epsilon_2} (\sigma_1 - \sigma_2). \quad (4)$$

Assuming uncorrelated errors in the measurement of σ_1 and σ_2 , one obtains the intermediate expression

$$\frac{\Delta\sigma_L}{\sigma_L} = \frac{1}{\epsilon_1 - \epsilon_2} \frac{1}{\sigma_L} \sqrt{\Delta\sigma_1^2 + \Delta\sigma_2^2}, \quad (5)$$

and by defining $R = \sigma_L/\sigma_T$ and $\Delta\sigma/\sigma = \Delta\sigma_i/\sigma_i$ and assuming $\Delta\sigma_1/\sigma_1 = \Delta\sigma_2/\sigma_2$, one obtains

$$\frac{\Delta\sigma_L}{\sigma_L} = \frac{1}{\epsilon_1 - \epsilon_2} \frac{\Delta\sigma}{\sigma} \sqrt{(1/R + \epsilon_1)^2 + (1/R + \epsilon_2)^2}. \quad (6)$$

Equation 6 demonstrates the error amplification due to the limited ϵ range and possibly small R . For the proposed measurements $R \leq 1$. The limited ϵ lever arm is the secondary source of error amplification. However, kinematic settings with significantly larger values of $\Delta\epsilon$ are not possible with the given beam energies, and the SHMS+HMS combination. The total

uncorrelated errors between high and low ϵ settings, which are dominated by kinematic and cross section model uncertainties, are listed in Table III. Given the significant error amplification for uncorrelated errors, the correlated systematic errors of a few percent can effectively be ignored. The last two columns in Table III list the correlated systematic errors assuming that the proposed measurement is carried out as one of the first experiments and assuming that it would run after the new spectrometer is well understood.

The ratio of longitudinal and transverse cross sections is not well known above the resonance region. As illustrated in Figure 1, theoretical predictions for σ_T disagree in magnitude by factors of 3-5. The longitudinal cross section predicted by the VGL Regge model for $Q^2=1.25 \text{ GeV}^2$ is on the order of $0.07 \mu\text{b}/\text{GeV}^2$ at $x_B=0.11$, resulting in L/T ratios of ≈ 1.24 . In this model, this ratio has a relatively strong W dependence as illustrated in figure 2. This ratio becomes smaller as x_B decreases, making Rosenbluth separations difficult due to the unfavorable error propagation. Predictions based on a parametrization based on previous kaon production data predict a transverse cross section larger by a factor of up to ~ 4 , which gives a L/T ratio of ≈ 0.2 . Recent separated cross section data from Hall C hint that transverse contributions are indeed larger than anticipated in the VGL model or other theoretical models.

The VGL Regge model by Vanderhaeghen, Guidal and Laget [1] provides a globally good description of the longitudinal $K^+\Lambda$ cross section for the available relatively low Q^2 data over an extended range of $-t$. However, σ_T is significantly underpredicted. Other available models also fail to describe the magnitude of the transverse cross section. For the rate estimation we have used the cross section predictions from the VGL Regge model as the parametrizations based on previous kaon electroproduction data are limited to a kinematic region outside of our proposed kinematics. Using a conservative approach, we used the empirical kaon production parametrization shown in figure 12.

The low $-t$ data at $Q^2=0.40, 1.25, 2.00$, and 3.00 GeV^2 in the proposed measurement will provide L-T separated data above the resonance region to determine the contributions of σ_L and σ_T for both Λ and Σ^0 final states. These data will provide important information about the K and K^* contributions to σ_L . If the data indicate that the $K^+\Lambda$ final state is dominated by the former, we will use these data to extract the kaon form factor, as has been done for π^+ production. The projected uncertainties of the Q^2 dependence of such a kaon form factor extraction are shown in figure 13. To investigate the normalization of the kaon form factor, we will also take a data point at the very low $Q^2=0.4 \text{ GeV}^2$ setting, which is in close proximity to the elastic e - K scattering kaon form factor results from CERN.

The L-T separated data at fixed values of $x_B=0.25$ and 0.40 will be used for tests of the onset of the $1/Q^n$ scaling in strange systems. To illustrate the sensitivity of the experiment, the projected uncertainties of the Q^2 dependence of the K^+ longitudinal cross section is shown in Figure 14. The filled symbols indicate the proposed K^+ measurement. We assume at least 1,000 good events for the $x_B=0.25$ and 800 good events for the $x_B=0.40$ for each ϵ setting to

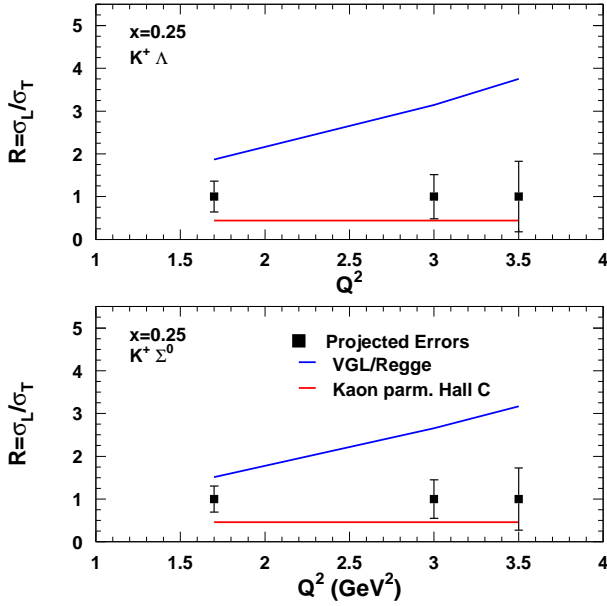


FIG. 12: The ratio of longitudinal and transverse cross sections, $R = \sigma_L/\sigma_T$, as calculated using the VGL Regge model as used in this proposal (blue solid) and a parametrization based on existing Hall C data (red solid). The error bars denote the uncertainty using a value for R as predicted by our parametrization. The VGL Regge model underpredicts σ_T at low Q^2 and W , but it is expected to become increasingly more accurate at larger Q^2 and W . Nevertheless, our estimates conservatively assume that the Regge calculation still underpredicts the transverse cross section even at the highest Q^2 point. Note that the proposed Q^2 points (filled symbols) were placed arbitrarily at unity. For the rate estimates in this proposal, we used our kaon parametrization based on previous Hall C data.

TABLE IV: The projected uncertainty in the fitting exponent in the Q^n dependence.

x_B	dn
0.25	0.4
0.40	0.5

determine the Q^2 dependence of the reaction. The uncertainties on the proposed points have been estimated using the VGL Regge model for both longitudinal and transverse cross sections, assuming a systematic uncertainty of 2.1% in the unseparated cross section, and correlated uncertainties as listed in Table III. The projected uncertainty in the fitting exponent in the Q^n dependence are listed in table IV. It should be emphasized that the projected uncertainty on dn depends on the projected uncertainty for σ_L , which in turn depends on the value of $R=\sigma_L/\sigma_T$. For consistency with the existing data we have used R values predicted in the VGL Regge model. One can see that it is feasible to accurately determine the Q^2 dependence with the proposed measurement.

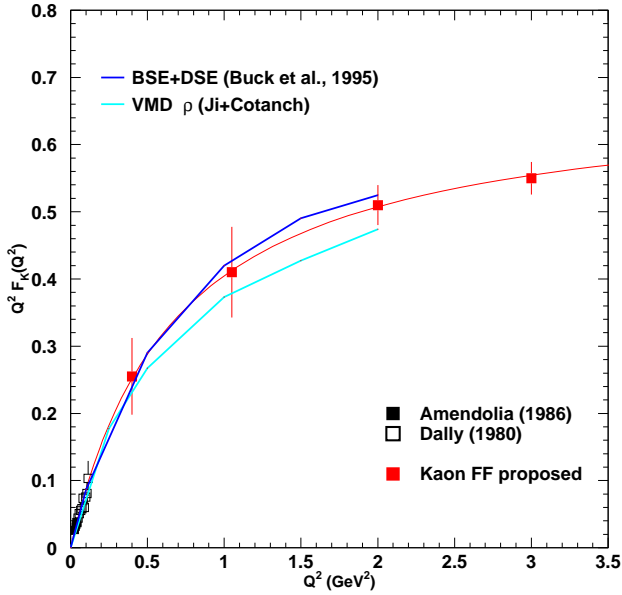


FIG. 13: *Projected uncertainties for the Q^2 dependence of the extracted kaon form factor if the data show that the extraction is warranted.*

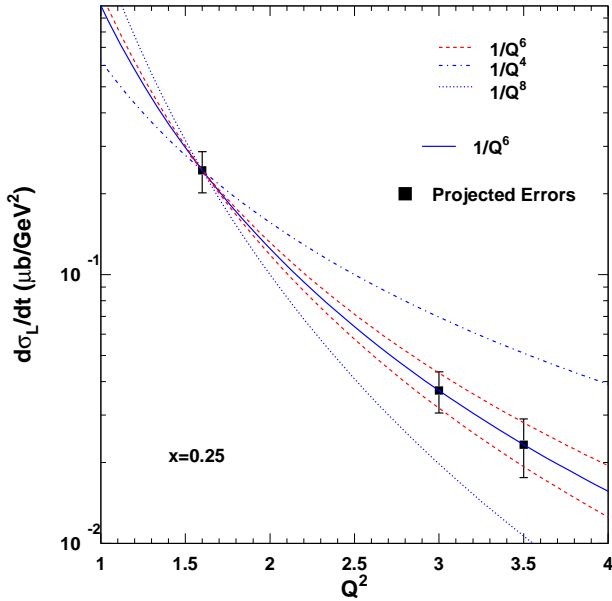


FIG. 14: *Projected uncertainties for the Q^2 dependence of σ_L at $x_B=0.25$.*

The resulting beam time estimate is listed in Table V. Note that the projected final uncer-

TABLE V: Beam time estimates for the $p(e, e' K^+) \Lambda (\Sigma^0)$ measurement assuming 90 μA on a 8-cm LH2 target. For the lowest Q^2 settings 35 μA on a 4-cm LH2 target was assumed. The projected number of hours includes three θ_K settings at high ϵ and two θ_K settings at intermediate and low ϵ .

Q^2 (GeV 2)	x_B	ϵ	LH2 hours	Dummy hours	Overhead (hours)	Total (hours)
0.40	0.072	0.411	114.1	7.7	4	125.8
0.40	0.072	0.692	75.3	5.2	4	84.5
1.25	0.122	0.477	16.5	1.2	4	21.7
1.25	0.122	0.696	13.0	0.9	4	17.9
2.00	0.182	0.396	53.7	3.7	4	61.4
2.00	0.182	0.584	30.0	2.1	4	36.1
2.00	0.182	0.751	29.7	2.1	4	35.8
3.00	0.250	0.393	93.8	6.6	4	104.4
3.00	0.250	0.689	65.5	4.6	4	74.1
Subtotal reaction mech.			491.6	34.1	36.0	561.7 (23.4 days)
1.70	0.249	0.587	24.8	1.7	4	30.5
1.70	0.249	0.858	14.6	1.1	4	19.7
3.50	0.250	0.357	56.3	0.4	4	60.7
3.50	0.250	0.555	47.2	0.3	4	51.5
Subtotal $x_B=0.25$			142.9	3.5	16.0	162.4 (6.8 days)
3.00	0.401	0.634	12.0	0.8	4	16.8
3.00	0.401	0.887	7.2	0.5	4	11.7
4.40	0.400	0.480	36.6	2.6	4	43.2
4.40	0.400	0.734	26.0	1.8	4	31.8
5.50	0.400	0.366	96.2	6.7	4	106.9
5.50	0.400	0.560	83.3	5.8	4	93.1
Subtotal $x_B=0.40$			261.3	18.2	24.0	303.5 (12.6 days)
Subtotals						1027.6
Calibrations						48.0
beam energy changes						48.0
Total						1123.6 (46.8 days)

tainties depend strongly on the ratio of longitudinal to transverse cross sections. For example, if R were half the assumed size, the uncertainty on σ_L would be reduced by a factor of two. The L/T ratios assumed in the estimate are listed in Table I. These are significantly smaller than those indicated by previous measurements. We thus expect that it is realistic to achieve the projected uncertainties in this experiment.

Our total time request is for 42.8 days of data, but additional time (≈ 4 days) will be

needed for calibration purposes and beam energy changes. Configuration changes have already been included in the time estimate in Table V. For example:

- $H(e, e')p$ elastic data and normalization checks ≈ 16 hours
- Spectrometer calibrations ≈ 16 hours
- Optics calibrations requiring ≈ 16 hours
- Energy and pass changes ≈ 48 hours

The experiment will require three different linac energies and eight pass changes. We assume an additional 8 hours overhead for each linac energy change and 4 hours for each pass change. The experiment will make use of the SHMS+HMS spectrometers in Hall C and require a (non-standard) 8-cm cryogenic hydrogen target. This target will also be used for two other 12 GeV approved experiments [38, 39].

IV. SUMMARY

In summary, we propose to use the SHMS and HMS spectrometers in Hall C to perform L-T separations of the $p(e, e', K^+) \Lambda, \Sigma^0$ reactions over a broad region of Q^2 and x_B . These will be the first high quality L-T separations for exclusive strangeness production from the proton above the resonance region.

We propose to acquire low $-t$ data at $Q^2=0.40, 1.25, 2.00$ and 3.00 GeV 2 to better understand the K^+ production mechanism, which at present suffers from large theoretical and experimental uncertainties. In particular, we aim to determine the contributions of σ_L and σ_T for both the Λ and Σ^0 final states. This would elucidate the role of K and K^* exchange contributions (in the t -channel). Because of the lack of precision data to aid model development, it is not yet established that K^+ electroproduction can be used to determine the kaon form factor, in analogy to the use of π^+ production to determine the pion charge form factor. If the data indicate that σ_L for the $K^+\Lambda$ final state is dominated by the K^+ pole at low $-t$, these data could be used (with an appropriate model) to extract the kaon form factor. A comparison of the $Q^2=0.40$ GeV 2 data with the form factor determined exactly at the CERN SPS will provide a necessary form factor consistency check, while the data up to $Q^2=3.0$ GeV 2 could provide the first extraction of the kaon form factor at higher Q^2 . These data would be of intense theoretical interest.

We also propose to acquire L-T-separated data at fixed values of $x_B=0.25$ and 0.40 , up to $Q^2=5.5$ GeV 2 , to investigate the onset of $1/Q^n$ scaling in strange systems. These would be the highest Q^2 for any L-T separations in kaon electroproduction, and would constrain the values of Q^2 for which one can reliably apply perturbative QCD concepts and extract Generalized Parton Distributions. This could influence the accessible kinematics for other GPD studies planned with the 12 GeV upgrade, and may help identify possible missing elements in existing calculations.

The experimental method proposed here has been successfully used in previous measurements in Hall C. A measurement of the $p(e, e'K^+)\Lambda$ reaction in the resonance region ($W=1.84$ GeV) [2] was among the first experiments performed in Hall C after the HMS and SOS were commissioned, and provided a significant constraint to model building [1]. The situation here is similar. The anticipated characteristics of the proposed SHMS+HMS spectrometers are well suited for the proposed measurements, and the quality of data obtained even relatively soon after the commissioning of the SHMS would be a huge advance in our present knowledge of K^+ production above the resonance region. These measurements require the construction of aerogel Čerenkov detectors to provide reliable K^+ identification over the intended momentum range, and we are confident that if this experiment is approved, funds will be found for this purpose.

- [1] M. Guidal, J.M. Laget, and M. Vanderhaeghen, Phys. Rev. C **61** 025204 (2000).
- [2] R.M. Mohring, et al., Phys. Rev. C **67** (2003) 055205.
- [3] M. Guidal, J.-M. Laget, M. Vanderhaeghen, Nucl. Phys. **A 627** (1997) 645.
- [4] T. Horn, et. al., Phys. Rev. Lett **97** 192001 (2006).
- [5] S.R. Amendolia, et al., Nucl. Phys. **B 277** (1986) 168; Phys.Lett. **B146** (1984) 116.
- [6] S.R. Amendolia, et al., Phys. Lett. **B 146** (1974) 116.
- [7] C.J. Bebek, et al., Phys. Rev. D **15**, 594 (1977).
- [8] J.-M.. Laget, private communication (2007).
- [9] M.M. Kaskulov, K. Gallmeister, U. Mosel, arXiv:0804.1834 [hep-ph].
- [10] O. Nachtmann, Nucl. Phys. **B74** 422 (1974).
- [11] A. Bartl and W. Majorotto, Nucl. Phys. **B55**, 493 (1975).
- [12] S.R. Brodsky, G.R. Farrar, Phys.Rev.Lett. **31** (1973) 1153.
- [13] T. Horn, et. al., Phys. Rev. C **78**, 058201 (2008).
- [14] O. Nachtmann, Nucl. Phys. **B115** 61-81 (1976).
- [15] V. Tadevosyan, et al., Phys. Rev. C **75**, 055205 (2007).
- [16] C. Hadjidakis, et al., Phys.Lett. **B605** 256-264 (2005).
- [17] M. Guidal *et al.*, arXiv:0711.3743.v1 (2008).
- [18] L. Morand, et al., Eur.Phys.J.**A24**, 445-458 (2005).
- [19] M.A. Shupe *et al.*, Phys. Rev. **D19**, 1921 (1979).
- [20] A. Danagoulian *et al.*, Phys. Rev. Lett.**98**, 152001 (2007).
- [21] K. Joo, M. Ungaro, C. Weiss, V. Kubarovský and P. Stoler, Hard Exclusive Electroproduction of π^0 and η with CLAS12, JLab 12 GeV Proposal PR12-06-101, 2006.
- [22] C.N. Brown, et al., Phys. Rev. Lett. **28** (1972) 1086.
- [23] C.J. Bebek, et al., Phys. Rev. Lett. **32**, 21 (1974).
- [24] P. Brauel, et al., Z. Phys. **C3**, 101 (1979).
- [25] P. Markowitz, et al., Electroproduction of Kaons up to $Q^2=3$ (GeV/c) 2 , proposal to Jefferson Lab PAC14 (E98-108).

- [26] P. Markowitz, et al., in preparation.
- [27] J.W.C. McNabb, et. al., Phys. Rev. C **69** 042201 (2004).
- [28] R.K. Bradford, et. al., Phys. Rev. C **73** 035202 (2006).
- [29] D.S. Carman, et al., Phys. Rev. Lett. **90** 131804 (2003).
- [30] B.A. Raue and D.S. Carman, Phys. Rev. C **71** 065209 (2005).
- [31] P. Ambrozewicz, et. al., Phys. Rev. C **57** 045203 (2007).
- [32] G. Huber, et al., Phys. Rev. C **78** 045203 (2008).
- [33] M.E. Christy, et al., Phys. Rev. C **70** 014206 (2004).
- [34] G. Huber, SHMS Heavy Gas Čerenkov Detector Design, April 1, 2002.
- [35] J. O'Connell and J. Lightbody, Comp. in Phys., May-June **57**, (1998).
- [36] wiser.f by Steve Rock, Wiser fit of proton, pion and kaon cross sections.
- [37] H.P. Blok, et al., Phys. Rev. C **78** 045202 (2008).
- [38] G. Huber et al., *Measurement of the Charged Pion Form Factor to High Q^2* , TJNAF Proposal E12-06-101, 2006.
- [39] T. Horn et al., *Scaling Study of the L-T Separated Pion Electroproduction Cross Section at 11 GeV*, TJNAF Proposal E12-07-105, 2007.

APPENDIX A: ADDITIONAL ϵ SETTINGS AND TOTAL UNCERTAINTY

It has been suggested that including additional beam energies in fitting σ_L and σ_T could improve the overall systematic uncertainty of the separated cross sections. We have thus performed a study to investigate the impact on our proposed experiment by evaluating the benefit of multiple ϵ settings, also considering the effect of systematic and statistical uncertainties. This is an important consideration, because additional ϵ settings naturally require additional beam time. The latter can be alleviated by, for instance, assuming that if one uses three ϵ settings, the statistics are re-distributed over a larger number of points. However, the resulting benefit in the systematic uncertainty has to be weighted carefully against the increased statistical uncertainty.

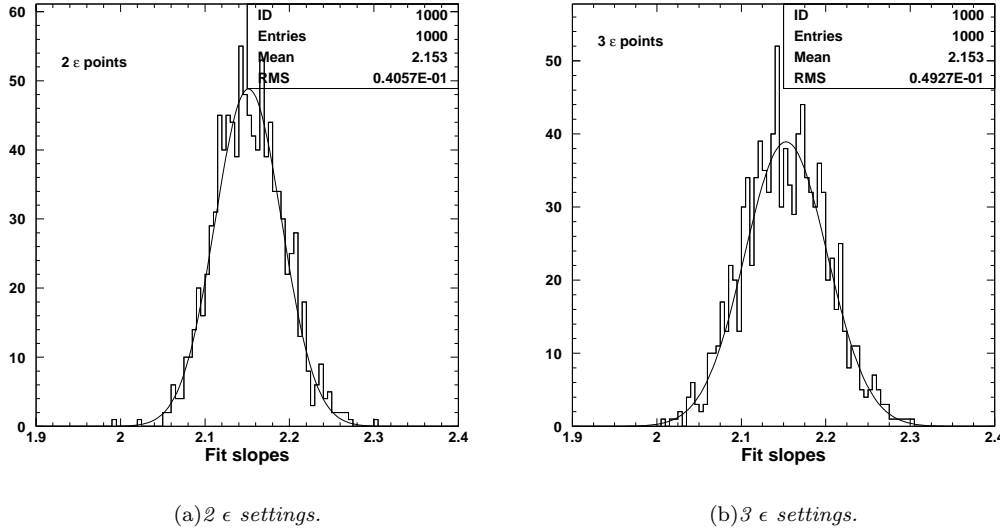


FIG. 15: *Fitted slope distributions from $\sigma_T + \epsilon\sigma_L$ at fixed Q^2 and W for 2ϵ and 3ϵ settings. A statistical uncertainty of about 2% was assumed for each data point in the 2ϵ points fit. In the case of three ϵ settings, it was assumed that the statistics are redistributed over a larger number of points, and so the total uncertainty was increased on each point. To get the same width as for 2ϵ points, one would have to increase the statistics by 15% for 3ϵ and by 67% for 5ϵ points.*

Figure 15 illustrates the merit of two vs. three epsilon settings in fitting σ_T and σ_L from $\sigma_T + \epsilon\sigma_L$. In this study, a statistical uncertainty of 1.9% was assumed on each point. To estimate the improvement in the fit by adding more points, fits were performed for 2, 3, and 5 ϵ settings. Next, the needed statistics for 2 ϵ points were re-distributed over 3 and 5 ϵ points reducing the statistics accordingly, and the fits were repeated. By comparing the resulting width of the fitted slopes for two ϵ settings with small uncertainty to those for 3 or 5 ϵ settings with large uncertainty, one can estimate the relative benefit.

From the fit slope width comparison, one can see that three points would provide a moderate improvement in the overall uncertainty, while the benefit of five epsilon points would be limited

TABLE VI: *Aerogel Čerenkov indices of refraction for this experiment. The number of photoelectrons expected within the spectral range of a 5" reference PMT are indicated for both K^+ and p , assuming a 10 cm aerogel radiator and conservative light collection efficiency.*

p_{MS} (GeV/c)	n	$K_{p.e.}$	$p_{p.e.}$
2.6-3.0	1.030	20-45	<0.5
3.1-3.7	1.020	12-30	<0.5
5.2-6.3	1.0075	6-13	<0.5
6.4-7.2	1.0055	6-9	<0.5

due to a significant increase in needed statistics.

APPENDIX B: CHARGED KAON IDENTIFICATION

The SHMS conceptual design report envisages the construction of one or more threshold aerogel Čerenkov detectors to provide reliable K^+/p separation over a wide momentum range. Although only one aerogel Čerenkov detector is required at any particular momentum, two detectors with differing indices of refraction (n) would reduce overhead to swap different n aerogels when changing SHMS momentum. Therefore, provision has been made in the SHMS detector stack for two threshold aerogel detectors, located in-between the heavy gas Čerenkov and the electromagnetic calorimeter. Unfortunately, these detectors have been descoped from the 12 GeV project, so funds for their construction would either have to be found from non-DOE sources, unused project contingency funds, or the Hall C operating budget.

The following is provided to indicate a means by which reliable kaon identification could be obtained over the required 2.6-7.1 GeV/c momentum range. Alternate methods are by no means excluded. In particular, the use of an aerogel RICH detector is a very interesting possibility for these momenta, and may ultimately be a better choice.

The design proposed here is based on the threshold aerogel detectors in the conceptual design report, supplementing the time of flight and coincidence timing cuts. In order to maintain good K^+/p separation, the index of refraction would have to be varied as indicated in Table VI. The number of photoelectrons is smallest for the lowest momentum of each range shown and increases with increasing momentum. After placement of a cut at 1.5 p.e. to eliminate knock-on events, a kaon detection inefficiency of less than 1% should be expected in most cases. Since the index of refraction has been selected so that protons do not produce Čerenkov radiation at any momentum, a K/p rejection ratio of at least 300:1, and possibly as high as 1000:1 should be possible.

Good K/π^+ separation is generally more straightforward. It can be accomplished for momenta >3.4 GeV/c by the heavy gas Čerenkov detector as illustrated in Figure 16. It is planned

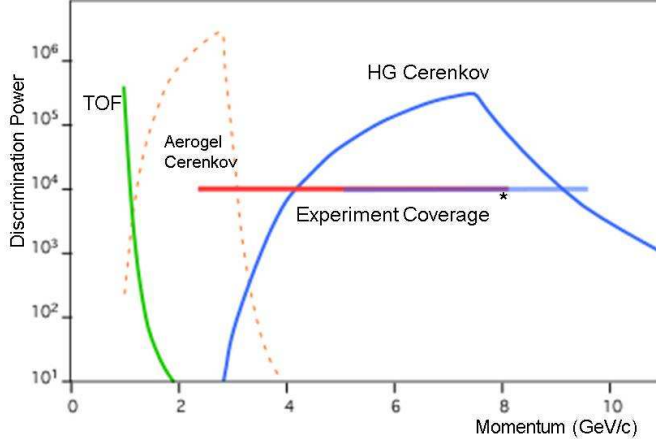


FIG. 16: π/K identification at positive polarity in the SHMS. The green solid line indicates particle identification via time of flight techniques, the orange dashed line denotes the kinematic coverage of the aerogel Čerenkov detector, and the solid blue line denotes the kinematic coverage of the heavy gas Čerenkov detector. The horizontal red line indicates the experimental requirements.

for the gas pressure to be reduced at higher momentum to ensure that kaons do not produce Čerenkov radiation, and so should achieve better than $10^4 K/\pi^+$ rejection at 8 GeV/c. Thus, particle identification should not be a problem in this region. However, care has to be taken in the design and construction of this detector so that the design goals are met. Good K/π^+ separation at lower momentum requires the use of one of the aerogel detectors.